ACS OMEGA

http://pubs.acs.org/journal/acsodf

Article

Preparation of Spherical HMX/DMF Solvates, Spherical HMX Particles, and HMX@NTO Composites: A Way to Reduce the Sensitivity of HMX

Huipeng Zhao,* Guanghui Gu, Jinjie Shen, Xinping Zhao, Jianlong Wang, and Guanchao Lan*

Cite This: *ACS Omega* 2023, 8, 14041−14046

Read Online

ACCESS | Metrics & More | Article Recommendations

ABSTRACT: To reduce the sensitivity of HMX (HMX = high-melting explosive—cyclotetramethylenetetranitramine), spherical HMX/DMF (DMF = dimethylformamide) solvates, spherical HMX particles, and HMX@NTO (NTO = 1,2,4-triazol-5-one) composites are prepared by crystallization. The structure and performance of spherical HMX crystals, HMX particles, and HMX@NTO composites are characterized by X-ray diffraction, Fourier-transform infrared spectroscopy, scanning electron microscopy, differential scanning calorimetry, accelerating rate calorimetry, and mechanical sensitivity test. The results show that the space group of the spherical HMX/DMF solvate is $\bar{R}3c$ with the lattice parameters of a = 15.9159(4) Å, b = 15.9159(4) Å, and c = 30.5136(8) Å. The non-isothermal stability and adiabatic thermal stability of HMX/DMF solvates are similar to those of HMX particles. The non-isothermal stability of HMX@NTO composites is lower than that of NTO and HMX particles, while the adiabatic thermal stability of HMX@NTO composites is higher than that of NTO but lower than that of HMX particles. The mechanical sensitivities of spherical HMX/DMF cocrystals, spherical HMX particles, and HMX@NTO composites are lower than that of raw HMX. This study can provide some guidance for desensitizing HMX and other energetic materials.

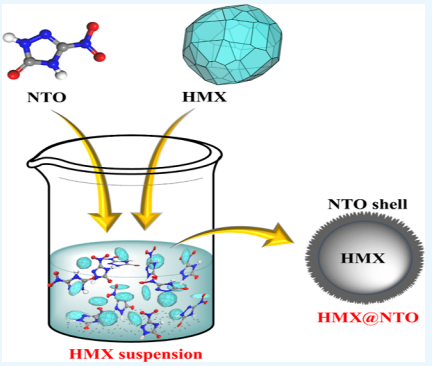

1. INTRODUCTION

High energy and low sensitivity are the two most significant requirements for energetic materials used in modern warhead. However, the existing high-energy materials usually exhibit poor sensitivity toward impact, friction, shock waves, thermal, and electric spark.[1] Therefore, it is an important job to design and prepare new energetic materials with high energy and low sensitivity or reduce the sensitivity of the existing high-energy materials. Compared with the development of new energetic materials, it is a more efficient method to reduce the sensitivity of high-energy explosives by physical or chemical methods.

During the past decades, considerable work has been done to decrease the sensitivity of conventional high-energy explosives through exploring energetic cocrystals,[2−5] improving the particle size and morphology,[6−9] and preparing energetic composites.[10−16] It is an effective strategy to decrease the high-sensitivity explosives by cocrystallization to introduce low-sensitivity or non-explosive components to high-sensitivity explosives. Cocrystals can bring about a completely different packing model of explosive molecules and thus lead to an alteration of key properties including the density, melting point, sensitivity, and detonation performance.[17] The crystal morphology plays an important role in determining the physical and chemical properties of energetic materials.[18,19] Compared with needle- or plate-shaped particles of energetic materials, spherical-shaped energetic materials have the advantages of lower sensitivity, better free-flowing properties, better mechanical properties, higher surface to volume ratio, higher packing density, higher bulk density, etc.[6] Therefore, the preparation of spherical energetic materials by recrystallization is another effective way to reduce the sensitivity of high-energy explosives. Preparing energetic composites via coating with polymers or low-sensitivity energetic materials has been widely used in desensitizing high-sensitivity explosives. This method can break the restriction for the incapability of changing the inherent molecules or components as compared with other approaches.[1]

A former study shows that HMX/DMF (HMX = high-melting explosive—cyclotetramethylenetetranitramine; DMF = dimethylformamide) solvates can be obtained by allowing a warm saturated solution of HMX in DMF to cool to room temperature.[20] In this study, spherical HMX/DMF solvates are obtained through recrystallization. Previous studies found that

Received: January 30, 2023
Accepted: March 10, 2023
Published: April 7, 2023

DMF molecules in HMX/DMF solvates can be easily removed through stirring in water.[18] When DMF molecules are removed from HMX/DMF solvates, spherical HMX particles with many gullies and holes can be obtained.[21] Generally, the surface of HMX crystals is smooth and adsorption sites on a smooth surface are less, which is not beneficial for the preparation of HMX-based composite explosives, especially for coating with low-sensitivity explosives. However, HMX particles with many gullies and holes are beneficial for the adsorption of low-sensitivity explosives. 1,2,4-Triazol-5-one (NTO) is an energetic material with low sensitivity that can decrease the sensitivity of HMX when NTO is deposited in the gullies and holes of HMX.

In this study, spherical HMX/DMF solvates, spherical HMX particles, and HMX@NTO composites are first prepared to decrease the sensitivity of HMX. The spherical HMX particles with many gullies and holes have wide potential applications in the preparation of HMX-based composites. The improvement in the surface roughness of spherical HMX particles and HMX@NTO composites provides an additional benefit to the adhesion of HMX crystals in energetic composites, which can be utilized for further practical applications.

2. EXPERIMENTAL DETAILS

2.1. Materials. HMX and NTO, provided by Gansu Yin Guang Chemical Industry Group Co. Ltd, were purified by recrystallization, and their mass fraction purity was greater than 0.99. DMF, acetic acid, and sodium lauryl sulfonate were of analytical grade and purchased from a local reagent factory without further purification.

2.2. Preparation of Spherical HMX/DMF Solvates. 10 g HMX samples were dissolved in 100 mL DMF at 85 °C under stirring. Then, 0.5 g of sodium lauryl sulfonate and 20 mL of acetic acid were added into the resulting solution and stirred at 85 °C until sodium lauryl sulfonate was completely dissolved. Subsequently, 10 mL of deionized water was dripped into the resulting solution and stirred for 30 min at 85 °C. Then, 0.5 g of HMX seed crystals was added when the resulting solution was cooled to 80 °C and stirred for 2 h at 80 °C. Then, the suspension was cooled to 20 °C with a cooling rate of 2.5 °C·h^{-1}. The suspension was filtered and washed with cold deionized water. Then, transparent spherical HMX/DMF solvates with a particle size (D_{50}) of 326.09 μm were obtained (Figure 1a).

2.3. Preparation of Spherical HMX Particles. Generally, the surface of HMX crystals is smooth as a result of the crystallization process, which makes it difficult for NTO particles to be adsorbed on the surface of HMX to prepare HMX@NTO composites. However, HMX particles with many gullies and holes are conducive to the adsorption of NTO particles during the coating process. The DMF of HMX/DMF solvates can be easily removed through stirring in water. HMX with a high specific surface area can be obtained by removing DMF in HMX/DMF solvates. Spherical HMX/DMF solvates (10 g) are added to 100 mL of deionized water and heated to 50 °C with stirring for 2 h to remove DMF from HMX/DMF solvates. Then, the spherical HMX particles (Figure 1b) with many gullies and holes can be obtained. The particle size (D_{50}) of HMX particles is 293.68 μm.

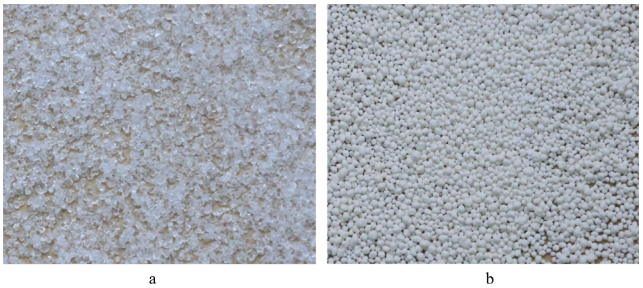

Figure 1. a) Spherical HMX/DMF solvates. (b) Spherical HMX particles.

2.4. Preparation of HMX@NTO Composites. NTO (4 g) is added to 100 mL of deionized water and heated to 50 °C with stirring for 30 min to make sure that NTO particles are completely dissolved. Subsequently, 10 g of spherical HMX particles is added to the resulting NTO solution, and then, the suspension is cooled to 20 °C with a cooling rate of 10 °C·h^{-1}. The dissolved NTO will precipitate from solution during cooling, and the precipitated NTO crystal will be adsorbed on the gullies and holes of HMX particles to form HMX@NTO composites. Then, they are filtered and washed with cold deionized water. The obtained HMX@NTO composites are dried in a vacuum oven at 50 °C for 8 h. The abovementioned procedures are repeated three times to increase the content of NTO. The particle size (D_{50}) of HMX@NTO composites is 363.82 μm.

2.5. Characterization of HMX/DMF Solvates, HMX Particles, and HMX@NTO Composites. The structures of HMX/DMF solvates, HMX particles, and HMX@NTO composites were characterized by powder X-ray diffraction (PXRD, X'Pert PRO MPD Diffractometer) and Fourier-transform infrared (FT-IR, Bruker VERTEX 80) spectroscopy. Single-crystal X-ray diffraction (SXRD, Bruker D8 Venture) was further used to identify the structure of HMX/DMF solvates. The crystal morphology of the HMX/DMF solvate was characterized by optical microscopy. The micro-surface topographies of HMX/DMF solvates, HMX particles, and HMX@NTO composites were characterized by scanning electron microscopy (SEM, Zeiss Sigma 300). Differential scanning calorimetry (DSC) and accelerating rate calorimetry (ARC, NETZSCH ARC 254) were used to study the non-isothermal decomposition property and adiabatic decomposition property of HMX/DMF solvates, HMX particles, and HMX@NTO composites. The impact sensitivity and friction sensitivity of HMX/DMF solvates, HMX particles, and HMX@NTO composites were measured to evaluate their mechanical safeties according to GJB 772A (GJB 1997).[22]

3. RESULTS AND DISCUSSION

3.1. Structure Characterization of Spherical HMX Solvates, HMX Particles, and HMX@NTO Composites. The crystal form and chemical structures of spherical HMX crystals, HMX particles, and HMX@NTO composites are characterized by PXRD and FT-IR, and the characterization results are summarized in Figure 2. PXRD patterns and FT-IR spectra of spherical HMX crystals are different from those of β-HMX, illustrating that the new crystal form or cocrystal is formed during the crystallization process of HMX in DMF. SXRD is further used to study the crystal structure of spherical HMX crystals. SXRD results show that the spherical HMX crystal is the HMX/DMF solvate. The space group of the HMX/DMF solvate is $\bar{R}3c$ with the lattice parameters of a = 15.9159(4) Å, b = 15.9159(4) Å, and c = 30.5136(8) Å, and 18 molecules of HMX and DMF are in the unit cell (Figure 3).

https://doi.org/10.1021/acsomega.3c00606
ACS Omega 2023, 8, 14041−14046

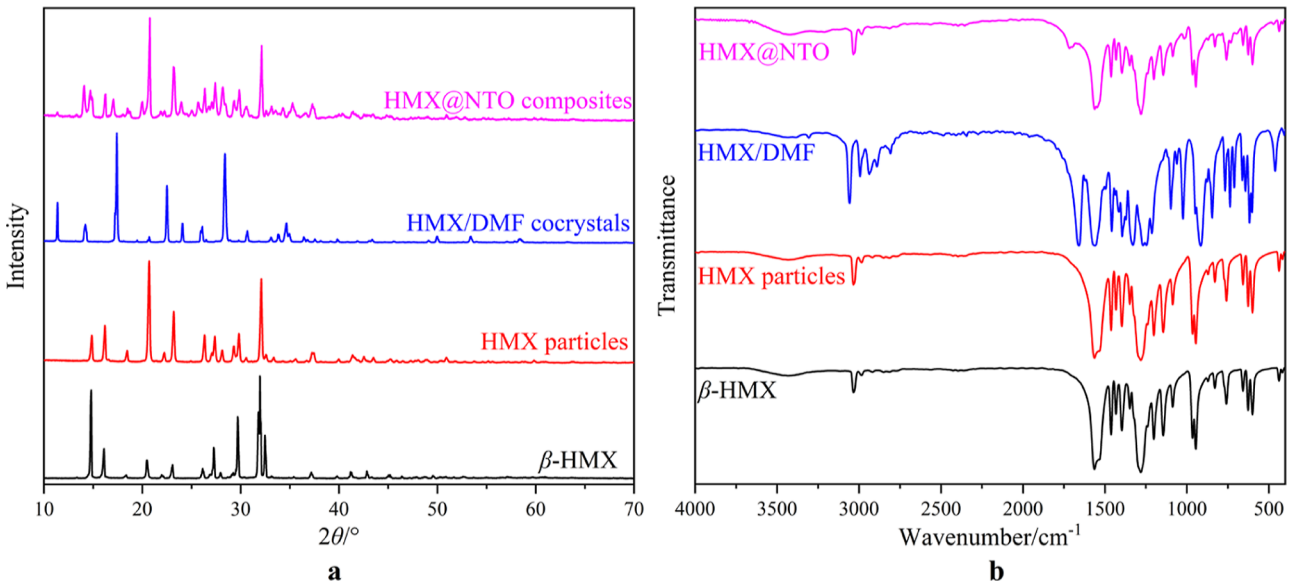

Figure 2. XRD patterns (a) and FT-IR spectra (b) of HMX particles, HMX/DMF solvates, and HMX@NTO composites.

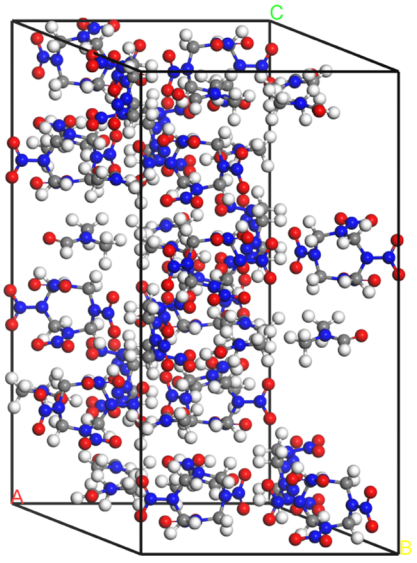

Figure 3. Crystal structure of HMX/DMF solvates.

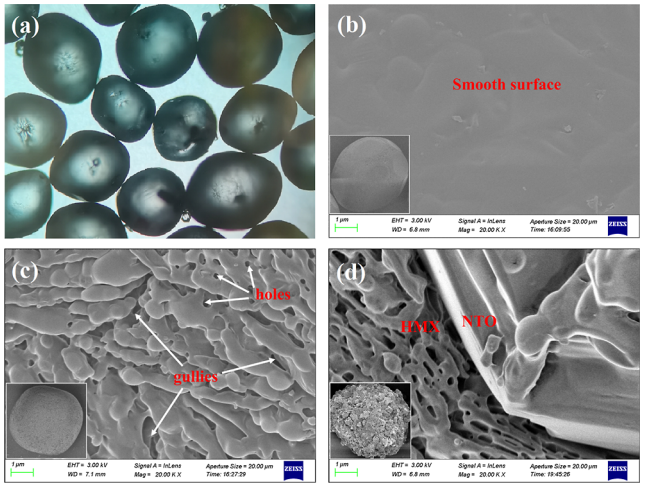

Figure 4. Macroscopic crystal morphology of HMX/DMF solvates (a), micro-surface topographies of HMX/DMF solvates (b), HMX particles (c), and HMX@NTO composites (d).

The crystal structure of the HMX/DMF solvate obtained from this study is the same as that of ref 20. The PXRD patterns and FT-IR spectra of HMX particles are the same as those of β-HMX, illustrating that β-HMX particles can be obtained by removing DMF from HMX/DMF solvates. For HMX@NTO composites, the characteristic peaks of β-HMX still exist, illustrating that the crystal form and chemical structure of β-HMX are not changed. In addition, the characteristic peaks of NTO emerge on the PXRD patterns, and FT-IR spectra of HMX@NTO composites illustrate that NTO has been introduced to HMX.

3.2. Morphology and Micro-surface Topographies of HMX/DMF Solvates, HMX Particles, and HMX@NTO Composites. The macroscopic crystal morphology and micro-surface topography of HMX/DMF solvates are characterized by optical microscopy and SEM, respectively, and the results are depicted in Figure 4a,b. It can be seen from Figures 1a,4a,b that the particle size of HMX/DMF solvates is homogeneous, and each HMX/DMF solvate presents a spherical shape, and the surface of the HMX/DMF solvate is smooth as a result of the crystallization process. The obtained spherical HMX/DMF solvates have many merits such as uniform texture, few crystal deficiencies, good dispersion, etc. As HMX particles and HMX@NTO composites are opaque, optical microscopy is unsuitable for characterizing their macroscopic morphologies. The micro-surface topographies of HMX particles and HMX@NTO composites are characterized by SEM, and the results are depicted in Figure 4c,d, respectively. Figure 4c illustrates that the micro-surface topography of HMX particles is much different from that of the HMX/DMF solvate. Many gullies and holes emerge on HMX particle surfaces due to the escape of DMF, resulting in greater roughness of HMX particles. The gullies and holes can provide many adsorption sites for NTO deposition, which is beneficial for the preparation of HMX@NTO composites and other HMX-based composites. Figure 4d illustrates that the micro-surface topography of HMX@NTO composites is much different from that of HMX particles. NTO crystals are

https://doi.org/10.1021/acsomega.3c00606
ACS Omega 2023, 8, 14041−14046

embedded in the gullies and holes of HMX particles. However, the particle size of NTO crystals is bigger than the size of gullies and holes on HMX particles, in that NTO crystals will grow up during the cooling process. If the coating time is sufficient, NTO will form a uniform shell on the HMX surface. Such an improvement in surface roughness of spherical HMX particles and HMX@NTO composites provide additional benefits to the adhesion of HMX crystals in energetic composites.

3.3. Non-isothermal Decomposition of HMX/DMF Solvates, HMX Particles, and HMX@NTO Composites. The non-isothermal decomposition properties of HMX/DMF solvates, HMX particles, and HMX@NTO composites are characterized by DSC at different heating rates under a nitrogen atmosphere. The obtained DSC results of HMX/DMF solvates, HMX particles, and HMX@NTO composites at a heating rate of 10 °C·min^{-1} are summarized in Figure 5.

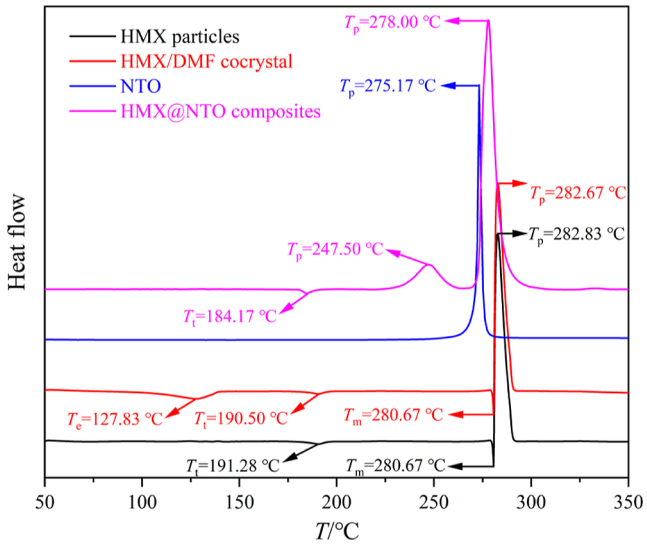

Figure 5. DSC results of HMX/DMF solvates, HMX particles, NTO, and HMX@NTO composites.

The decomposition temperature (T_p) of different samples at different heating rates are summarized in Table 1. Based on DSC results, the activation energy is obtained by Kissinger and Ozawa methods.[23,24]

Table 1. Decomposition Temperature and Activation Energy of Different Samples, T_p/°C

heating rate/°C·min−1	Tp/°C			
	HMX	NTO	HMX/DMF	HMX@NTO
5	278.59	271.35	278.66	244.11
10	282.83	275.17	282.67	247.50
15	284.40	276.94	284.17	249.31
20	285.32	279.19	285.21	251.24
Ea/(kJ·mol^{-1})	493.98	436.40	513.68	430.7

For HMX/DMF solvates, there is an endothermic peak (T_e = 127.83 °C) on the DSC curve, which represents DMF escape from the HMX/DMF solvate lattice. When DMF is removed from HMX/DMF solvates, β-HMX particles are obtained. The phase-transition temperature (T_t), melting point (T_m), and decomposition temperature (T_p) of HMX/DMF solvates are essentially in agreement with those of HMX particles, illustrating that DMF has few influences on the non-isothermal stability of HMX in HMX/DMF solvates. Compared with HMX particles, the T_t of HMX@NTO composites decreases from 191.28 to 184.17 °C, illustrating that NTO reduces the stability of β-HMX. For HMX@NTO composites, the T_p of NTO decreases from 275.17 to 247.50 °C, illustrating that the non-isothermal stability of NTO is decreased. For pure NTO, the intermediate products and heat generated by NTO decomposition can be immediately blown away by N_2, resulting in a low self-acceleration effect. For HMX@NTO composites, some intermediate products and heat are sealed in the gullies and holes of HMX, which can rapidly accelerate the decomposition of NTO, thus reducing the T_p of NTO. In addition, the lower onset decomposition and T_p of NTO are also favored by smaller particulate domains trapped in the holes of HMX particles. The solid residue of NTO decomposition is adsorbed on the gullies and holes of HMX particles, which can catalyze the decomposition process of HMX, thus reducing the T_p of HMX from 282.83 to 278.00 °C. Above all, the non-isothermal stability of HMX/DMF solvates is the same as that of HMX particles, while the non-isothermal stability of HMX@NTO is lower than that of HMX particles.

3.4. Adiabatic Thermal Decomposition of HMX/DMF Solvates, HMX Particles, and HMX@NTO Composites. As DSC-obtained results are seriously affected by measurement conditions, ARC is further used to study the adiabatic thermal decomposition of HMX/DMF solvates, HMX particles, and HMX@NTO composites. Samples (120 ± 1 mg) are measured using the heat-wait-search (HWS) procedure with a temperature increase of 5 °C.[25,26] Compared with DSC, ARC can measure much more samples, and the decomposition process obtained by ARC is controlled by the sample rather than forced from an outside temperature program. Therefore, ARC can be used to obtain the properties of HMX/DMF solvates, HMX particles, and HMX@NTO composites themselves. The obtained exothermic processes of HMX/DMF solvates, HMX particles, NTO, and HMX@NTO composites are summarized in Figure 6. The obtained initial decomposition temperature (T_0), initial decomposition time (t_0), final decomposition temperature (T_f), final decomposition

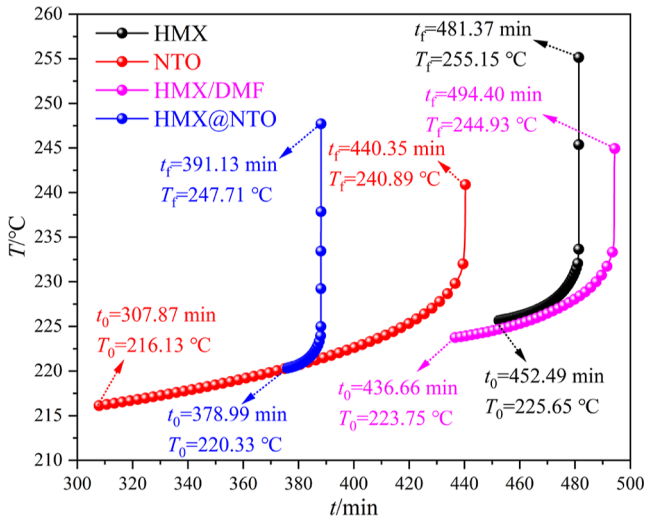

Figure 6. ARC results of HMX/DMF solvates, HMX particles, NTO, and HMX@NTO composites.

https://doi.org/10.1021/acsomega.3c00606
ACS Omega 2023, 8, 14041−14046

time (t_f), adiabatic temperature rise (ΔT_{ad}), maximum temperature rise rate (β_m), and whole decomposition period (Δt) are listed in Table 2.

Table 2. Adiabatic Thermal Decomposition Parameters of HMX/DMF Solvates, HMX Particles, NTO, and HMX@NTO Composites

parameters	HMX particles	NTO	HMX/DMF	HMX@NTO
sample mass/g	0.1202	0.1207	0.1204	0.1206
T_0/°C	225.65	216.13	223.75	220.33
t_0/min	452.49	307.87	436.66	378.99
T_f/°C	255.15	240.89	244.93	247.71
t_f/min	481.37	440.35	494.40	391.13
ΔT_{ad}/°C	29.50	24.76	21.18	27.38
Δt/min	28.88	132.48	57.74	12.14

The ARC measurement results demonstrate that the T_0 of HMX/DMF solvates is close to that of HMX particles, illustrating that the adiabatic thermal stabilities of HMX/DMF solvates and HMX particles are close. During the ARC measurement process, HMX/DMF solvates will first absorb heat to remove DMF and form HMX particles, which is an endothermic process that cannot be detected by the ARC instrument. Subsequently, the formed HMX particles continue to decompose. The decomposition period (Δt) of HMX/DMF solvates is longer than that of HMX particles. The adiabatic temperature rise (ΔT_{ad}) of HMX/DMF solvates is lower than that of HMX particles, in that some HMX particles are replaced by non-explosive component DMF in solvates. The T_0 of HMX@NTO composites is higher than that of NTO but lower than that of HMX, illustrating that the adiabatic thermal stability of HMX@NTO composites is between NTO and HMX. For HMX@NTO composites, NTO is embedded in the gullies and holes of HMX, resulting in a close contact between NTO and HMX. Therefore, the heat can be conducted to HMX particles, when NTO suffers external thermal stimulations. For ARC measurements, the intermediate products and heat produced by NTO or HMX@NTO composites are sealed in the sample cell, and thus, the catalytic effects are the same, which is different from DSC measurements (performed with perforated cups). When NTO starts decomposition, many intermediate products will be produced and thus catalyze the decomposition of HMX. Therefore, the decomposition period of HMX@NTO is shorter than that of HMX particles.

3.5. Mechanical Sensitivities of HMX/DMF Solvates, HMX Particles, and HMX@NTO Composites. The impact sensitivity and friction sensitivity of raw HMX, HMX/DMF solvates, spherical HMX particles, and HMX@NTO composites are measured using GJB 772A to evaluate their mechanical safety. The obtained mechanical sensitivities are summarized in Table 3.

Table 3. Impact Sensitivity and Friction Sensitivity of Raw HMX, HMX/DMF Solvates, HMX Particles, and HMX@NTO Composites

parameters	raw HMX	HMX/DMF	HMX particles	HMX@NTO
impact sensitivity/%	100	12	72	44
friction sensitivity/%	100	8	64	40

It can be concluded from Table 3 that the mechanical sensitivities of HMX/DMF solvates are significantly decreased after spheroidization cocrystallization treatments. On the one hand, the introduction of non-explosive component DMF completely changes the packing model of HMX molecules and thus leads to an alteration of sensitivity. DSC results show that DMF escape temperature is lower than HMX decomposition temperature, illustrating that HMX/DMF solvates will absorb much energy to remove DMF when suffering external mechanical stimulation, thus significantly decreasing the mechanical sensitivities. On the other hand, there are few edges and corners on spherical HMX/DMF solvates, resulting in the fact that the external mechanical stimulation can evenly act on spherical HMX/DMF solvates, resulting in a uniform stress dispersion, thus decreasing the probability of hot spot formation. The mechanical sensitivities of spherical HMX particles are lower than that of raw HMX because of the better free-flowing property and particle gradation of spherical HMX particles. However, the mechanical sensitivities of spherical HMX particles are higher than that of spherical HMX/DMF solvates because of no non-explosive component in spherical HMX particles and the rough surface together with more defects of spherical HMX particles. The mechanical sensitivities of HMX@NTO composites are lower than that of raw HMX and spherical HMX particles, in that the insensitive NTO can share some stress when suffering external mechanical stimulation. Moreover, some gullies and holes of HMX are filled by NTO, which can decrease the probability of hot spot formation. Above all, the mechanical sensitivity of HMX can be decreased by preparing spherical HMX/DMF solvates, spherical HMX particles, and HMX@NTO composites.

4. CONCLUSIONS

Spherical HMX/DMF solvates, spherical HMX particles, and HMX@NTO composites are obtained, and the mechanical sensitivity of HMX is significantly decreased. The space group of the spherical HMX/DMF solvate is $\bar{R}$-3c with the lattice parameters of a = 15.9159(4) Å, b = 15.9159(4) Å, and c = 30.5136(8) Å, and 18 molecules of HMX and DMF are in the unit cell. The crystal form of HMX particles does not change during the preparation of HMX@NTO composites. The surface of spherical HMX/DMF solvates is smooth with few defects. The surface of spherical HMX particles is rough, and many gullies and holes exist on HMX particles. For HMX@NTO composites, NTO is embedded in the gullies and holes of HMX particles. The non-isothermal stability and adiabatic thermal stability of HMX/DMF solvates are similar to those of HMX particles. The non-isothermal stability of HMX@NTO composites is lower than that of NTO and HMX particles, while the adiabatic thermal stability of HMX@NTO composites is higher than that of NTO but lower than that of HMX particles. The mechanical sensitivities of spherical HMX/DMF solvates, spherical HMX particles, and HMX@NTO composites are lower than that of raw HMX, illustrating that the sensitivity of high-energy explosives can be decreased by cocrystallization, improving morphology and preparing composites.

https://doi.org/10.1021/acsomega.3c00606
ACS Omega 2023, 8, 14041−14046

AUTHOR INFORMATION

Corresponding Authors

Huipeng Zhao − *School of Chemistry and Chemical Engineering, North University of China, Taiyuan 030051, China*; Email: 490163142@qq.com

Guanchao Lan − *School of Chemistry and Chemical Engineering, North University of China, Taiyuan 030051, China; Gansu Yin Guang Chemical Industry Group Co. Ltd., Baiyin 730900, China;* orcid.org/0000-0002-8059-2602; Email: gclan@nuc.edu.cn

Authors

Guanghui Gu − *Gansu Yin Guang Chemical Industry Group Co. Ltd., Baiyin 730900, China*

Jinjie Shen − *Gansu Yin Guang Chemical Industry Group Co. Ltd., Baiyin 730900, China*

Xinping Zhao − *Gansu Yin Guang Chemical Industry Group Co. Ltd., Baiyin 730900, China*

Jianlong Wang − *School of Chemistry and Chemical Engineering, North University of China, Taiyuan 030051, China*

Complete contact information is available at: https://pubs.acs.org/10.1021/acsomega.3c00606

Notes

The authors declare no competing financial interest.

ACKNOWLEDGMENTS

This work wass supported by the Scientific and Technological Innovation Programs of Higher Education Institutions in Shanxi (grant no. 2019L0606) and the Fundamental Research Program of Shanxi Province (grant no. 202103021223201).

REFERENCES

(1) Yang, Z.; Ding, L.; Wu, P.; Liu, Y.; Nie, F.; Huang, F. Fabrication of RDX, HMX and CL-20 based microcapsules via in situ polymerization of melamineformaldehyde resins with reduced sensitivity. *Chem. Eng. J.* **2015**, *268*, 60−66.

(2) Sun, S.; Zhang, H.; Liu, Y.; Xu, J.; Huang, S.; Wang, S.; Sun, J. Transitions from separately crystallized CL-20 and HMX to CL-20/HMX cocrystal based on solvent media. *Cryst. Growth Des.* **2018**, *18*, 77−84.

(3) Bolton, O.; Matzger, A. J. Improved stability and smart-material functionality realized in an energetic cocrystal. *Angew. Chem., Int. Ed.* **2011**, *123*, 9122−9125.

(4) Lin, H.; Zhu, S. G.; Li, H. Z.; Peng, X. H. Synthesis, characterization, AIM and NBO analysis of HMX/DMI cocrystal explosive. *J. Mol. Struct.* **2013**, *1048*, 339−348.

(5) Lin, H.; Zhu, S. G.; Li, H. Z.; Peng, X. H. Structure and detonation performance of a novel HMX/LLM-105 cocrystal explosive. *J. Phys. Org. Chem.* **2013**, *26*, 898−907.

(6) Mandal, A. K.; Thanigaivelan, U.; Pandey, R. K.; Asthana, S.; Khomane, R. B.; Kulkarni, B. D. Preparation of spherical particles of 1,1-diamino-2,2-dinitroethene (FOX-7) using a micellar nanoreactor. *Org. Process Res. Dev.* **2012**, *16*, 1711−1716.

(7) Shang, F.; Zhang, J. A Successive and scalable process for preparing spherical submicrometer-sized RDX by the SEDS process. *J. Energ. Mater.* **2014**, *32*, S71−S82.

(8) Zhao, X.; He, D.; Ma, X.; Liu, X.; Xu, Z.; Chen, L.; Wang, J. Preparation, characterization of spherical 1,1-diamino-2,2-dinitroethene (FOX-7), and study of its thermal decomposition characteristics. *RSC Adv.* **2021**, *11*, 33522−33530.

(9) Xu, W.; Wang, J.; Peng, J.; Liang, X.; Li, H.; Wang, J. Study on the influencing factors of ultrafine spherical RDX during spray drying with low speed. *J. Nanomater.* **2019**, *2019*, 1−10.

(10) Lan, G.; Zhang, G.; Shen, J.; Li, Z.; Wang, J.; Li, J. Establishing the interface layer on the pentaerythritol tetranitrate surface *via in situ* reaction. *Langmuir* **2022**, *38*, 12016−12023.

(11) Liu, T. K.; Luh, S. P.; Perng, H. C. Effect of boron particle surface coating on combustion of solid propellants for ducted rockets. *Propell. Explos. Pyrot.* **1991**, *16*, 156−166.

(12) Gong, F.; Zhang, J.; Ding, L.; Yang, Z.; Liu, X. Mussel-inspired coating of energetic crystals: A compact core-shell structure with highly enhanced thermal stability. *Chem. Eng. J.* **2017**, *309*, 140−150.

(13) Lan, G.; Zhang, G.; Shen, J.; Jin, G.; Wang, J.; Li, J. Ameliorating the sensitivities, thermal and combustion properties of RDX by in situ self-assembly TA-Pb/Cu shells to RDX surface. *Arab. J. Chem.* **2023**, *16*, 104497.

(14) Li, Z.; Zhao, X.; Gong, F.; Lin, C.; Liu, Y.; Yang, Z.; Nie, F. Multilayer deposition of metal-phenolic networks for coating of energetic crystals: modulated surface structures and highly enhanced thermal stability. *ACS Appl. Energy Mater.* **2020**, *3*, 11091−11098.

(15) Zhang, S.; Kou, K.; Zhang, J.; Jia, Q.; Xu, Y. Compact energetic crystals@urea-formaldehyde resin micro-composites with evident insensitivity. *Compos. Commun.* **2019**, *15*, 103−107.

(16) Lan, G.; Jin, G.; Ruan, J.; Zhao, X.; Wang, J.; Li, J. Establishing TA-Pb/Cu and SA-Pb/Cu interface catalyst shells on HMX surfaces via in situ coprecipitation to ameliorate the performances of HMX. *Arab. J. Chem.* **2023**, *16*, 104720.

(17) Wang, Y.; Yang, Z.; Li, H.; Zhou, X.; Zhang, Q.; Wang, J.; Liu, Y. A novel cocrystal explosive of HNIW with good comprehensive properties. *Propell. Explos. Pyrot.* **2013**, *35*, 1−7.

(18) Salvalaglio, M.; Vetter, T.; Giberti, F.; Mazzotti, M.; Parrinello, M. Uncovering molecular details of urea crystal growth in the presence of additives. *J. Am. Chem. Soc.* **2012**, *134*, 17221−17233.

(19) Li, J.; Jin, S.; Lan, G.; Ma, X.; Ruan, J.; Zhang, B.; Chen, S.; Li, L. Morphology control of 3-nitro-1,2,4-triazole-5-one (NTO) by molecular dynamics simulation. *Crystengcomm* **2018**, *20*, 6252−6260.

(20) Cobbledick, R. E.; Small, R. W. H. The crystal structure of the complex formed between 1,3,5,7-tetranitro-1,3,5,7-tetraazacyclooctane (HMX) and *N*,*N*-dimethylformamide (DMF). *Acta Cryst* **1975**, *31*, 2805−2808.

(21) Liu, Y.; Xu, J.; Huang, S.; Li, S.; Wang, Z.; Li, J.; Jia, J.; Huang, H. Microstructure and performance of octahydro-1,3,5,7-tetranitro-1,3,5,7-tetrazocine (HMX) crystal clusters obtained by the solvation-desolvation process. *J. Energ. Mater.* **2019**, *37*, 282−292.

(22) *GJB 772A. Explosive test method*, Beijing, China Weapons Industry Press, 1997.

(23) Kissinger, H. E. Reaction kinetics in differential thermal analysis. *Anal. Chem.* **1957**, *29*, 1702−1706.

(24) Ozawa, T. A new method of analyzing thermogravimetric data. *B. Chem. Soc. JPN.* **1965**, *38*, 1881−1886.

(25) Lan, G.; Jin, S.; Chen, M.; Li, J.; Lu, Z.; Wang, N.; Li, L. Preparation and performances characterization of HNIW/NTO-based high-energetic low vulnerable polymer-bonded explosive. *J. Therm. Anal. Calorim.* **2020**, *139*, 3589−3602.

(26) Lan, G.; Zhang, G.; Chao, H.; Li, Z.; Wang, J.; Li, J. Ameliorating the performances of 3,4-bis(4′ -nitrofurazano-3′ -yl)-furoxan (DNTF) by establishing tannic acid (TA) interface layer on DNTF surface. *Chem. Eng. J.* **2022**, *434*, 134513.

https://doi.org/10.1021/acsomega.3c00606
ACS Omega 2023, 8, 14041−14046